Available online at www.sciencedirect.com
ScienceDirect
Russian Geology and Geophysics 52 (2011) 1353–1367
RUSSIAN GEOLOGY AND GEOPHYSICS
www.elsevier.com/locate/rgg

H_2O and CO_2 in parental magmas of Kliuchevskoi volcano inferred from study of melt and fluid inclusions in olivine

N.L. Mironov [a,*], M.V. Portnyagin [a,b]

[a] *V.I. Vernadsky Institute of Geochemistry and Analytical Chemistry (GEOKHI), Russian Academy of Sciences, ul. Kosygina 19, Moscow, 119991, Russia*
[b] *Leibniz Institute of Marine Research, IFM-GEOMAR, Wischhofstrasse 1-3, 24148 Kiel, Germany*

Received 17 February 2011; accepted 5 April 2011

Abstract

This paper reports new FTIR data on the H_2O and CO_2 concentrations in glasses of 26 naturally quenched and experimentally partially homogenized melt inclusions in olivine ($Fo_{85–91}$) phenocrysts from rocks of the Kliuchevskoi volcano. Measured H_2O concentrations in the inclusions range from 0.02 to 4 wt.%. The wide variations in the H_2O content of the inclusions, which do not correlate with the host olivine composition and contents of major elements in the melts, are explained by the H_2O escape from inclusions via diffusion through the host olivine during the magma eruption and the following cooling. The largest H_2O loss is characteristic of inclusions from lava samples which cooled slowly after eruption. The minimal H_2O loss is observed for inclusions from rapidly quenched pyroclastic rocks. Parental magmas of the Kliuchevskoi volcano are estimated to contain 3.5 wt.% H_2O. The new data imply a 40 °C lower mantle temperatures than that estimated earlier for the Kliuchevskoi primary melts. The concentrations of CO_2 in glasses range from <0.01 to 0.13 wt.% and do not correlate with the type of studied inclusions and their composition. The calculated pressures of melt equilibria with H_2O–CO_2 fluid inside the inclusions are lower than 270 MPa. They are significantly lower than a pressure of 500 MPa calculated from the density (~0.8 g/cm^3) of cogenetic fluid inclusions in high-Fo olivine. The significant pressure drop inside the melt inclusions after their trapping in olivine might be due to the H_2O loss and redistribution of CO_2 from melt to daughter fluid phase. Compared with melt inclusions, cogenetic fluid inclusions provide independent information about the crystallization pressures of olivine and initial CO_2 content in the Kliuchevskoi magma, which were estimated to be at least 500 MPa and 0.35 wt.%, respectively. The maximum CO_2 concentrations in the primary Kliuchevskoi melts are estimated at 0.8–0.9 wt.%. The decompression crystallization of the Kliuchevskoi magmas starts at depths of 30–40 km and proceeds with a continuous decrease in CO_2 content and an increase (up to 6–7 wt.%) and then a decrease (at <300 MPa) in H_2O content in melts, which explains the origin of the whole spectrum of rocks and melt inclusions of the Kliuchevskoi volcano.

Keywords: melt and fluid inclusions in olivine; parental magmas; H_2O; CO_2; Kliuchevskoi volcano; Kamchatka

Introduction

Studies of melt and fluid inclusions are of paramount importance for the understanding of the physicochemical conditions of formation and evolution of magmas (Metrich and Wallace, 2008; Naumov, 2011; Smirnov et al., 2011; Sokolova et al., 2011). H_2O and CO_2 are major volatile components of magmas, which is fundamental in magmatic processes. They influence the melting of the mantle, the composition of magmas and their crystallization, the nature of volcanic eruptions and climate (Carroll and Holloway, 1994). During the past decade, there has been a significant increase in the number of studies of volatiles in magmas formed in a subduction-related setting, especially those concerned with melt inclusions in minerals (Naumov et al., 2010). Much less attention has been paid to the question of the representativeness of glass compositions of melt inclusions for characterization of the initial concentration of H_2O and CO_2 in magmas (Danyushevsky et al., 2002; Metrich and Wallace, 2008; Portnyagin et al., 2008). These studies have shown that the processes occurring in inclusions after their entrapment in host mineral can significantly change the initial content of H_2O and CO_2 in melt inclusions. Underestimating the effect of these processes leads to an incorrect interpretation of data on the content of volatiles in inclusions and wrong petrological conclusions.

In this work, we performed a systematic study of H_2O and CO_2 contents in melt and fluid inclusions in high-magnesian

* Corresponding author.
E-mail address: nmironov@geokhi.ru (N.L. Mironov)

1068-7971/$ - see front matter © 2011, V.S. Sobolev IGM, Siberian Branch of the RAS. Published by Elsevier B.V. All rights reserved.
doi:10.1016/j.rgg.2011.10.007

olivine from rocks of the Kliuchevskoi volcano using IR spectroscopy and cryometry. The data are used to discuss the evolution of H_2O and CO_2 contents in melt inclusions and conformity between the results for cogenetic melt and fluid inclusions, as well as to estimate the possible initial concentrations of H_2O and CO_2 in magmas of the Kliuchevskoi volcano.

Characterization of samples studied and inclusions in olivines

Composition of rocks and olivines of the Kliuchevskoi volcano. The Kliuchevskoi volcano 4750 m high with a volume of erupted magma of about 250 km^3 is the world-renowned and largest volcano in Eurasia. It is located in the Central Kamchatka Depression in the northern part of the Eastern Kamchatka volcanic belt, whose magmatism is associated with the subduction of the Pacific plate beneath Kamchatka and the melting of the mantle wedge under the influence of fluids separating from the subducted plate (Portnyagin et al., 2007b). The Kliuchevskoi volcano is part of the Kliuchevskoi group of volcanoes, which is the largest in Kamchatka and includes 12 volcanoes, with a total volume of erupted rocks of about 5000 km^3 (Melekestsev, 1980) over the past ~300 ka (Calkins, 2004). The Kliuchevskoi volcano is the youngest among them; its age is about 7000 years (Braitseva et al., 1995). The minimum average annual magma output from the Kliuchevskoi volcano is 60 million tons, which makes it the most productive island-arc volcano in the world (Fedotov and Masurenkov, 1991).

The Kliuchevskoi volcano was the subject of many petrological and geochemical studies (Ariskin et al., 1995; Dorendorf et al., 2000; Mironov et al., 2001; Khubunaya et al., 1994, 2007; Kersting and Arculus, 1994; Khrenov et al., 1989; Ozerov, 2000; Portnyagin et al., 2007a,b). Issues related to the H_2O content of magmas of the Kliuchevskoi volcano were considered in papers (Churikova et al., 2007; Khubunaya and Sobolev, 1998; Mironov et al., 2001; Portnyagin et al., 2007b; Sobolev and Chaussidon, 1996), which give estimates of the H_2O content in melts and their sources based on ion probe measurements of H_2O. IR spectroscopy data on the H_2O and CO_2 contents in melt inclusions in olivine from the Kliuchevskoi volcano are given in (Auer et al., 2009).

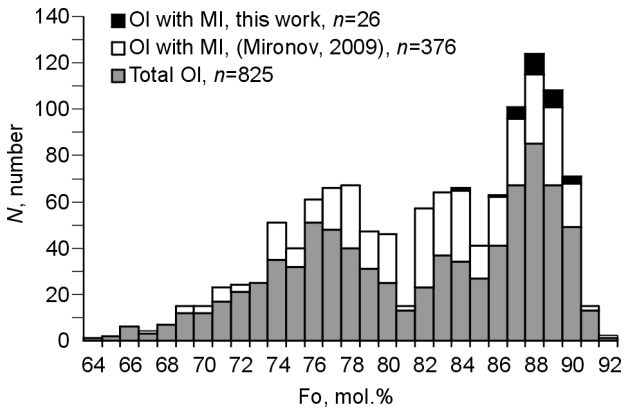

Fig. 1. Distribution of olivine phenocrysts (Fo) in Kliuchevskoi volcano rocks. The figure shows the composition of all phenocrysts and phenocrysts with melt inclusions (MIs) (Mironov, 2009). $Fo = 100 \cdot (Mg/(Mg + Fe^{2+}_{tot}))$.

Rocks of the Kliuchevskoi volcano form a continuous series from high-magnesian basalts to moderately magnesian high-alumina andesite-basalts of normal alkalinity (Ariskin et al., 1995). In this work, we studied samples of Cpx-Ol and Ol-Cpx-Pl porphyritic varieties of lavas and pyroclastics (bombs, scoria) of historic (Tuyla, Apakhonchich, Piipa) and older (Bulochka, Luchitskogo, Ochki) eruptions on the slopes of the volcano, which represent the full range of rock compositions of the Kliuchevskoi volcano. The chemical composition and a petrographic description of the samples studied are given in (Churikova et al., 2007; Dorendorf et al., 2000; Khubunaya et al., 1994; Portnyagin et al., 2007a,b).

Olivine phenocrysts are present in all types of rocks of the Kliuchevskoi volcano (Khubunaya et al., 1994; Kersting and Arculus, 1994). Its composition varies over a wide range from Fo_{92} to Fo_{65}. The presence of melt and more rare fluid inclusions is characteristic of the entire range of olivine compositions (Fig. 1, Table 1).

Melt and fluid inclusions in olivine. In this study, we investigated the largest inclusions in high-magnesian olivine (Fo > 85), which were previously analyzed for the content of major elements, trace elements, and volatiles (Portnyagin et al., 2007b; Churikova et al., 2007) (see Fig. 1, Table 1). Two types of magmatic inclusions, melt and fluid, were studied (Fig. 2).

Melt inclusions (MIs) are divided into two types: recrystallized inclusions (predominant type), which were previously investigated in homogenization experiments (see Fig. 2, *b*, *c*), and naturally quenched glassy inclusions (see Fig. 2, *a*). IR spectroscopy was subsequently performed on 23 inclusions of the first type ($Fo_{84.6–90.6}$) and three naturally quenched inclusions ($Fo_{86.4–90.4}$) (see Table 1).

Devitrified inclusions were usually large and single or, less commonly, multiple inclusions in a grain, with a smoothed olivine faceting (see Fig. 2, *b*, *c*). The size of the inclusions ranged from 55 to 165 μm (mean diameter, see Table 1). The inclusions varied in crystallinity from finely recrystallized (in samples of bombs and scoria) to coarsely recrystallized inclusions (in lava samples). The phase composition of the recrystallized inclusions was represented by association Cpx + glass + gas phase + Cr-Spl ± Al-Spl ± sulfide. The daughter phases in the inclusions have a high-alumina composition (e.g., Al_2O_3 = 7–15 wt.% in Cpx and 65 wt.% for Al-Spl), which clearly distinguishes them from phenocrysts and crystalline inclusions in minerals and is a consequence of specific, possibly metastable crystallization conditions in melt inclusions (Portnyagin et al., 2005). The gas phase of recrystallized inclusions was presented, as a rule, by one large bubble and smaller bubbles scattered among clinopyroxene crystals. The low density of the gas phase made it impossible to study its phase composition.

Glassy naturally quenched inclusions were found in olivine from a sample of volcanic sand of Apakhonchich lava

Table 1. Characteristics and composition (major elements and volatiles) of melt inclusions in olivine

Parameters and composition of glasses of MIs	1	2	3	4	5	6	7	8	9	10	11	12	13
	E289	E291-2	E295-1	E296-1	E299	E312-1	E314	E316-1	E318	E319-1	AP4	AP3	Ol20E
Flow/cone	Luchits-kogo	Luchits-kogo	Luchits-kogo	Luchits-kogo	Piipa	Bulochka	Bulochka	Bulochka	Bulochka	Bulochka	Apakhon.	Apakhon.	Apakhon.
Sample No.	KHUB-2	KHUB-2	KHUB-2	KHUB-2	PIKH	KHUB-5	KHUB-5	KHUB-5	KHUB-5	KHUB-5	AP1	AP1	AP1
Rock	HMB	HMB	HMB	HMB	HAB	HMB	HMB	HMB	HMB	HMB	HAB	HAB	HAB
Rock type	Bomb	Bomb	Bomb	Bomb	Bomb	Bomb	Bomb	Bomb	Bomb	Bomb	Scoria	Scoria	Scoria
T_{quench}, ºC	1190	1210	1182	1195	1145	1170	1190	1145	1145	1160	–	–	1252
MI diameter, μm	143	140	65	84	98	150	94	85	115	80	63	70	98
Bubble diameter, μm	73	N.d.	25	25	35	50	29	30	35	25	23	28	35
Bubble volume, rel.%	13.2		5.7	2.7	4.6	3.7	3.0	4.4	2.8	3.1	4.7	6.1	4.6
Host olivine, Fo	87.5	89.6	89.5	89.5	84.6	87.9	88.9	88.3	88.1	88.9	86.4	90.4	89.5
SiO_2, wt.%	51.12	49.10	47.03	49.48	49.72	51.33	49.50	49.38	48.81	48.95	48.07	50.88	47.51
TiO_2	0.98	0.82	0.92	0.80	1.03	0.96	0.84	0.87	0.95	1.08	1.10	1.05	0.69
Al_2O_3	16.23	14.80	16.52	14.17	17.39	15.17	14.47	15.65	15.91	16.53	18.18	17.12	12.66
FeO	7.41	6.34	6.80	6.89	7.76	6.63	6.81	7.57	7.66	6.92	7.32	4.98	7.60
MnO	0.12	0.09	0.13	0.13	0.15	0.13	0.09	0.12	0.14	0.09	0.12	0.07	0.13
MgO	8.23	9.35	8.82	9.92	7.13	8.59	9.59	8.30	7.85	8.10	5.33	5.54	12.41
CaO	9.83	14.44	13.44	12.81	10.26	9.83	12.23	12.21	11.77	11.65	12.24	13.87	12.17
Na_2O	2.99	2.25	2.57	2.33	3.46	3.12	2.54	2.65	2.79	3.02	3.51	3.06	1.99
K_2O	0.62	0.40	0.55	0.41	0.94	0.73	0.49	0.44	0.49	0.63	0.71	0.76	0.50
P_2O_5	0.13	0.10	0.14	0.07	0.17	0.20	0.16	0.08	0.16	0.13	0.20	0.17	0.14
Cl	0.04	0.06	0.11	0.06	0.06	0.09	0.08	0.06	0.06	0.09	0.14	0.09	0.10
S	0.09	0.19	0.25	0.20	0.21	0.09	0.19	0.17	0.19	0.15	0.32	0.19	0.21
Total	97.8	97.9	97.3	97.3	98.3	96.9	97.0	97.5	96.8	97.4	97.2	97.8	96.1
H_2O (SIMS), wt.%	2.80	2.80	2.37	1.91	2.47	3.06	2.66	2.37	2.67	2.35	2.31	1.32	2.68
Reference	P-07	P-07	P-07	P-07	P-07	P-07	P-07	P-07	P-07	P-07	P-07	P-07	P-07

Parameters and composition of glasses of MIs	14	15	16	17	18	19	20	21	22	23	24	25	26
	Ol5$_av	bul129-g1	bul144-g1	bul17-g1	bul27-g1	bul78-g1	o124-g1	o177-g1	o179-g1	o50-g1	t13-g1	t35-g2	t75-g1
Flow/cone	Apakhon.	Bulochka	Bulochka	Bulochka	Bulochka	Bulochka	Ochki	Ochki	Ochki	Ochki	Tuyla	Tuyla	Tuyla
Sample No.	AP1	KLU-98-01	KLU-98-01	KLU-98-01	KLU-98-01	KLU-98-01	KLU-96-03	KLU-96-03	KLU-96-03	KLU-96-03	KLU-96-15	KLU-96-15	KLU-96-15
Rock	HAB	HMB	HMB	HMB	HMB	HMB	MB	MB	MB	MB	MB	MB	MB
Rock type	Scoria	Lava	Lava	Lava	Lava	Lava	Lava	Lava	Lava	Lava	Lava	Lava	Lava
T_{que}, ºC	–	1214	1242	1214	1253	1220	1231	1315	1190	1258	1275	1267	1292
MI diameter, μm	168	90	155	104	165	69	85	78	78	88	86	75	55
Bubble diameter, μm	66	35	53	38	60	28	43	35	35	40	38	30	25
Bubble volume, rel.%	6.1	5.9	3.9	4.7	4.8	6.4	12.5	9.2	9.2	9.6	8.2	6.4	9.4
Host olivine, Fo	89.8	88.7	90.6	88.5	89.7	89.0	89.4	90.1	89.3	89.5	88.7	88.4	87.5
SiO_2, wt.%	50.22	48.49	47.33	48.3	47.81	47.58	48.99	48.82	49.2	50.31	50.17	48.51	49.26
TiO_2	0.92	1.08	0.76	1.04	0.93	0.97	0.9	0.81	1.17	0.9	0.91	0.99	0.98
Al_2O_3	15.85	18.64	16.34	18.37	15.59	17.57	17.89	16.09	19.2	16.35	15.99	16.94	16.02
FeO	5.51	6.30	6.25	6.50	7.56	5.97	4.98	5.23	4.43	4.87	5.94	6.03	7.06
MnO	0.08	0.09	0.1	0.12	0.16	0.1	0.08	0.09	0.08	0.09	0.11	0.1	0.12
MgO	6.20	8.25	9.66	8.18	10.85	8.73	9.03	12.19	7.31	10.23	10.1	10	10.95
CaO	13.22	13.78	16.06	13.08	12.76	14.74	14.52	13.21	13.58	14.36	11.96	12.63	11.78
Na_2O	2.74	3.28	2.47	3.41	2.78	2.97	3.01	2.86	3.95	2.89	3.43	3.28	3.19
K_2O	0.70	0.58	0.52	0.58	0.53	0.58	0.69	0.65	0.94	0.68	1.05	0.99	0.78
P_2O_5	0.16	0.16	0.09	0.14	0.11	0.12	0.13	0.1	0.18	0.13	0.2	0.21	0.18
Cl	0.11	0.08	0.08	0.07	0.08	0.09	0.09	0.09	0.11	0.09	0.11	0.11	0.06
S	0.15	0.12	0.12	0.08	0.16	0.11	0.08	0.12	0.06	0.12	0.16	0.15	0.16
Total	95.9	100.9	99.8	99.9	99.3	99.5	100.4	100.3	100.2	101.0	100.1	99.9	100.5
H_2O (SIMS), wt.%	2.34	0.13	0.10	0.33	0.99	0.13	0.07	0.06	0.12	0.07	0.06	0.06	0.08
Reference	P-07	Ch-07	Ch-07	Ch-07	Ch-07	Ch-07	Ch-07	Ch-07	Ch-07	Ch-07	Ch-07	Ch-07	Ch-07

Note. Contents of major elements, volatiles, and host olivine (Fo) are given from data by (Portnyagin et al., 2007b)—P-07 and (Churikova et al., 2007)—Ch-07. Rock type: HMB, MB, and HAB—high-magnesian, magnesian, and high-alumina basalts, respectively, from (Ariskin et al., 1995). Apakhon. means Apakhonchich. Melt inclusions O15$ (column 14) and o177-g1 (column 21) are shown on Fig. 2, *a* and Fig. 2, *d*, respectively.

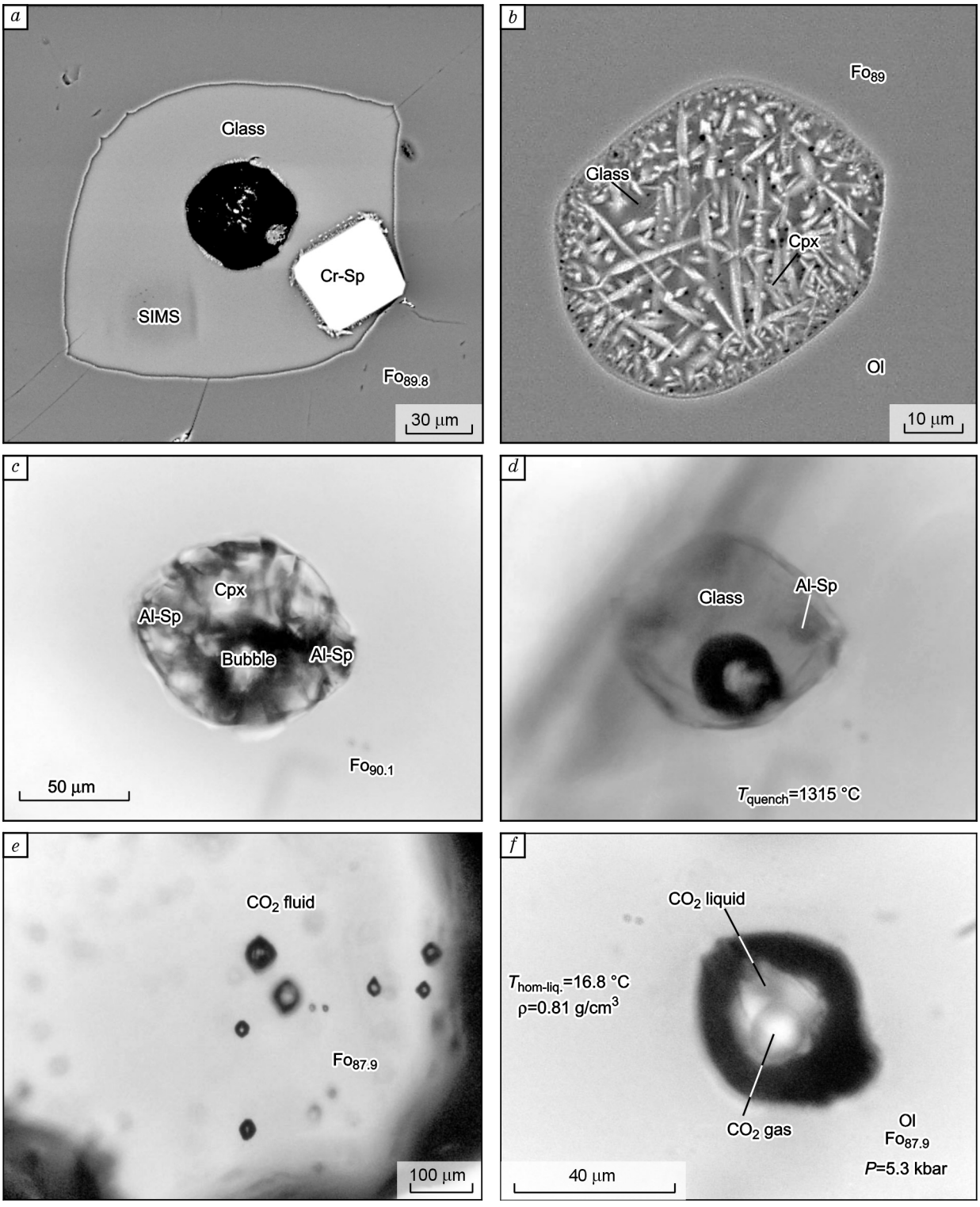

Fig. 2. Representative types of melt and fluid inclusions in magnesian olivine. *a–d*, Melt inclusions: *a*, naturally quenched glassy MI (Apakhonchich flow, Ol5$ inclusion, see Tables 1 and 2), *b*, one type of recrystallization of recrystallized MIs (Apakhonchich flow), *c*, *d*, recrystallized MI before and after the experiment (Ochki flow, o177 inclusion, see Tables 1 and 2); *e*, *f*, fluid inclusions of CO_2 (~ Fo_{88}, Ochki flow, o19 grain): *e*, general view of the distribution of inclusions in the grain, *f*, one of the large inclusions in this grain, close shot. The photomicrographs were taken in secondary electron (*a*, *b*) and polarized transmitted light (*c–f*).

flow. These inclusions consisted of glass, a gas bubble, and a prisoner spinel (see Fig. 2, *a*). The inclusions varied in size from 65 to 170 μm (see Table 1).

In high-magnesian olivines of the Kliuchevskoi volcano, *fluid inclusions* (FIs) are rare (Khubunaya et al., 2007), and we encountered them in Fo_{88} olivine grains (Ochki flow) (see Fig. 2, *e*, *f*) together with syngenetic melt inclusions (MI o19—Churikova et al., 2007). The investigated FIs consisted of a group of nine inclusions ranging in size from 5 to 45 μm (see Fig. 2, *e*). At room temperature of about

20 °C, the inclusions were single-phase and changed into two-phase inclusions upon cooling. The composition of the FIs is close to pure CO_2, as shown by an experimental cryometric study (see below).

Research methods

Experimental study of melt inclusions. Homogenization of partially crystallized melt inclusions was carried out on the Slutskii–Sobolev low-inertia high-temperature system for microscopic studies (Sobolev and Slutskii, 1984). Two-sided polished grains of olivine with internal inclusions were used. The experiments were performed in an atmosphere of high-purity helium at a pressure of 1 atm. The thermocouple was calibrated by the melting point of gold (T = 1064 °C); during the experiment, a small piece of gold foil was located on the surface of the investigated grain with an inclusion. The temperature range of the experiments (quenching temperature) was 1145–1315 °C (see Table 1). Complete homogenization (with the disappearance of the gas bubble) was not achieved in any of the experiments. As a rule, MIs were quenched at 10–20 °C above the melting point of the last daughter pyroxene crystal in the inclusion. The time at temperatures above 1000 °C was not more than 15 min to prevent possible loss of water from the MIs. High-water inclusions differed from low-water inclusions in lower temperature during active melting of daughter phases (1015–1045 °C and 1175–1190 °C, respectively), lower melt viscosity, which was evident from the velocity of motion of a gas bubble in an inclusion during the experiment, and complete melting of daughter crystals of pyroxene at lower temperature as compared with low-water inclusions (1180 °C and 1250 °C on average, respectively, see Table 1). Low-water inclusions were characterized by the presence of residual alumina spinel (see Fig. 2, *d*), which did not melt even at a significant rise in temperature obviously higher than the temperature of inclusions entrapment (up to 1320 °C).

Like naturally quenched inclusions, the inclusions quenched in the experiment consisted of glass, a gas bubble, and a spinel crystal. The constant presence of spinel in primitive inclusions appears to reflect the same mechanism of their entrapment in olivine involving the adhesion of a small crystal of chrome spinel to the face of the growing olivine crystal. The volume of the gas phase averaged 6.2% of the volume of inclusions after quenching in nature or in the experiment. Further studies showed that low-water (H_2O < 1 wt.%) inclusions had a systematically larger volume of the gas phase compared to high-water inclusions (H_2O > 1 wt.%) (7.5 and 5 vol.%, respectively) regardless of the quenching temperature (see Table 1).

Experimental study of fluid inclusions. To determine the composition and density, the FIs were examined using the experimental cryometric setup of Vernadsky Institute of Geochemistry and Analytical Chemistry (GEOKHI, RAS) using the procedure of (Naumov, 1979). The homogenization temperature (T_{hom}), i.e., the temperature of transition of CO_2 from the two-phase state (liquid + gas) to the single-phase state was determined by double or triple heating of FIs cooled below the homogenization temperature. The density of CO_2 for T_{hom} was determined using the model of (Span and Wagner, 1996). The pressure of entrapment in olivine was calculated for temperatures estimated independently from data of the liquidus thermometry of melt inclusions (T = 1200–1250 °C), using the equation of state of CO_2 from (Sterner and Pitzer, 1994). All calculations were performed using the spreadsheet from (Hansteen and Klügel, 2008).

All FIs in the grain studied (see Fig. 2, *e*) behaved the same way. After freezing of the inclusions, the melting point (–56.2 °C) was close to the temperature of the triple point (gas + solid phase + fluid phase) of pure CO_2 (–56.6 °C), indicating a negligible admixture of other components to CO_2 in the FI. All FIs were homogenized into liquid. For individual FIs, the interval of T_{hom} was 16.8–17.4 °C, which corresponds to a density of 0.805–0.800 g/cm^3. Cryometric study of FIs was performed before and after the experimental study of syngenetic melt inclusions in the grain. After a high-temperature experiment (heating to 1250 °C), the FIs had the same density as before the experiment.

Analysis of melt inclusions glasses by Fourier transform infrared spectroscopy (FTIR). For FTIR studies of melt inclusions (MIs), we prepared plates of individual grains of olivine containing MIs which were opened and polished on both sides. For this, grains with the largest inclusions analyzed previously by electron and ion probes were selected. Each grain was placed with the polished side down on an adhesive tape at the center of a plastic ring 2.5 cm in diameter, which was then filled with epoxy resin. The lower part of the epoxy mount with an olivine grain at the center was cut to a thickness of ~1 mm and glued onto a glass plate (~0.5 cm thick). The plate was ground using corundum abrasive papers with water until the appearance of another side of the inclusion on the surface, and was then polished with 6, 3, and 1 μm diamond pastes. The resulting plate of olivine grain with the inclusion was separated from the epoxide ring, glue, and glass holder using acetone and washed in ethanol and deionized water. The thickness of the plates fixed vertically on double-sided adhesive tape was measured under a microscope. The thickness of the plates varied from 100 to 25 μm, depending on the size of inclusions (see Table 2). For the analysis, the plates with MIs were put horizontally on the edge of a preparation glass coated with double-sided adhesive tape so that only a smaller part of a plate was stuck and the inclusion was surrounded by air on both sides. The preparation thus produced allow transport and storage of inclusions.

The CO_2 and H_2O content in glasses of melt inclusions were determined by Fourier transform infrared spectroscopy (FTIR) on a setup consisting of a Bruker IFS88 spectrometer and an IR-Scope II microscope at the Institute of Mineralogy at Leibniz University (Hannover, Germany). A detailed description of the method is presented in (Shishkina et al., 2010a).

CO_2 was analyzed in the mid-infrared regime (MIR) based on the intensity of the absorption peaks of CO_3^{2-} at wavenum-

Table 2. H_2O and CO_2 contents in glasses of melt inclusions according to IR spectroscopy data

No.	MI	Thickness, μm	Bubble inside	H_2O (SIMS), wt.%	Density, g/L	H_2O_{tot}, wt.% (3550 cm^{-1}) MIR	OH, wt.% (4500 cm^{-1}) NIR	H_2O_{mol}, wt.% (5200 cm^{-1}) NIR	H_2O_{tot}, wt.% NIR	H_2O (FTIR), wt.%	CO_2, wt.%			*P*, MPa	
											(1530 cm^{-1}) MIR	(1430 cm^{-1}) MIR	(average) MIR	NL-2002	Sh-2010
1	2	3	4	5	6	7	8	9	10	11	12	13	14	15	16
1	E289	60		2.80	2695	2.03	1.78	1.15	2.93	**2.93**	<0.01	**<0.01**	<0.01	<102	**<108**
2	E291-2	68	+	2.80	2695	1.78	1.70	1.07	2.76	**2.76**	0.0167	**0.0189**	0.0178	113	**117**
3	E295-1	33		2.37	2705	1.41	N.d.	N.d.	N.d.	**>1.41**	0.0222	**0.0249**	0.0236	90	**115**
4	E296-1	30		1.91	2715	1.75	N.d.	N.d.	N.d.	**>1.75**	0.0409	**0.0312**	0.0360	104	**109**
5	E299	60	+	2.47	2702	1.40	1.51	0.95	2.46	**2.46**	0.0180	**0.0146**	0.0163	90	**99**
6	E312-1	96	+	3.06	2689	1.43	1.99	1.98	3.97	**3.97**	0.0145	**0.0134**	0.0140	178	**167**
7	E314	30		2.66	2698	1.85	2.27	N.d.	> 2.27	**>2.27**	0.0429	**0.0429**	0.0429	162	**155**
8	E316-1	33		2.37	2705	2.03	2.03	N.d.	> 2.03	**>2.03**	0.0575	**0.0435**	0.0505	151	**146**
9	E318	48		2.67	2698	1.47	1.43	1.15	2.58	**2.58**	0.0150	**0.0129**	0.0139	91	**100**
10	E319-1	42		2.35	2705	1.19	N.d.	N.d.	N.d.	**>1.19**	<0.01	<0.01	<0.01	<78	**<89**
11	AP4	34		2.31	2706	1.42	N.d.	N.d.	N.d.	**>1.42**	<0.01	<0.01	<0.01	<79	**<89**
12	AP3	48		1.32	2728	0.91	N.d.	N.d.	N.d.	**>0.91**	N.d.	**0.0366**	0.0366	97	**104**
13	Ol20E	68	+	2.68	2698	1.58	1.52	1.02	2.53	**2.53**	0.1422	**0.1256**	0.1339	219	**269**
14	Ol5$_av	80		2.34	2705	1.46	1.53	0.98	2.52	**2.52**	0.0420	**0.0430**	0.0425	161	**154**
15	bul129-g1	42		0.13	2754	0.08	N.a.	N.a.	N.a.	**0.08**	< 0.01	**0.0108**	0.0108	19	**46**
16	bul144-g1	52		0.10	2755	0.04	N.d.	N.d.	N.d.	**0.04**	< 0.01	**0.0150**	0.0150	19	**53**
17	bul17-g1	68		0.33	2750	0.20	N.a.	N.a.	N.a.	**0.20**	0.0093	**0.0076**	0.0084	13	**41**
18	bul27-g1	98	+	0.99	2735	0.79	0.62	0.39	1.00	**1.00**	0.0326	**0.0274**	0.0300	48	**81**
19	bul78-g1	41		0.13	2754	0.08	N.d.	N.d.	N.d.	**0.08**	0.0148	**0.0184**	0.0166	25	**59**
20	o124-g1	50		0.07	2755	0.05	N.a.	N.a.	N.a.	**0.05**	0.0121	**0.0151**	0.0136	33	**53**
21	o177-g1	41		0.06	2756	0.05	N.a.	N.a.	N.a.	**0.05**	0.0297	**0.0297**	0.0297	59	**78**
22	o179-g1	48	+	0.12	2754	0.08	N.a.	N.a.	N.a.	**0.08**	0.0126	**0.0157**	0.0142	34	**54**
23	o50-g1	58	+	0.07	2755	0.05	N.a.	N.a.	N.a.	**0.05**	0.0104	**0.0130**	0.0117	28	**50**
24	t13-g1	31		0.06	2756	N.d.	N.a.	N.a.	N.a.	N.d.	<0.01	<0.01	< 0.01	<22	**<45**
25	t35-g2	26		0.06	2756	0.02	N.a.	N.a.	N.a.	**0.02**	0.0232	**0.0291**	0.0262	51	**77**
26	t75-g1	35		0.08	2755	N.d.	N.a.	N.a.	N.a.	N.d.	<0.01	<0.01	< 0.01	<22	**<45**

Note. The table gives data on H_2O and CO_2 contents in glasses of melt inclusions obtained by FTIR in different regimes and estimated pressures in the inclusions. The adopted values of the concentrations are in bold. For H_2O (column 11) these values correspond to the combination of data for NIR (columns 8–10) for high-water glasses and MIR (column 7) for low-water glasses. For CO_2, the values were obtained from the peaks of CO_3 at 1430 cm^{-1}. See explanations in the text. Two values of the pressure are given. NL-2002 pressures (column 15) were estimated using VolatileCalc 1.1 (Newman and Lowenstern, 2002) based on H_2O, CO_2, and SiO_2 contents and quenching temperature or the calculated temperature of equilibrium with the olivine for naturally quenched inclusions. For inclusions with underestimated water content according to FTIR, the calculation was performed using SIMS data. Sh-2010 pressures (column 16) were corrected using experimental data (Shishkina et al., 2010a) by the equation $P_{Sh\text{-}2010} = 34.929 + P_{NL\text{-}2002}/1.2698$ (see Fig. 8 in (Shishkina et al., 2010a)). N.d., Content was not determined due to technical difficulties (absence of peaks or the presence of noise in spectra due to the small thickness of the sample or insufficient area for analysis). N.a., Not analyzed.

bers of 1530 and 1430 cm^{-1} (Fig. 3, *a*, *b*). The H_2O content was estimated from the intensity of H_2O peak at 3550 cm^{-1} in the MIR (see Fig. 3, *a*). High contents of H_2O were also analyzed in the near-infrared regime (NIR) based on the total peak intensity of molecular H_2O at 5200 cm^{-1} and OH^- at 4500 cm^{-1} (the actual position of the peak of OH^- in the glasses was within 4500–4470 cm^{-1}) (see Fig. 3, *c*). In addition to the analysis of pure glasses, we also obtained several combined spectra for glasses and gas bubble inclusions in them (see Fig. 3, *a*). The size of the analysis area ranged from 300 to 3000 μm^2 and averaged about 1000 μm^2 (36×28 μm). We performed 70 measurements, of which the sharpest spectra were subsequently selected for quantitative calculations of H_2O and CO_2 concentrations.

The peaks of CO_3^{2-}, OH^-, molecular H_2O, and total H_2O, expressed in relative units of absorption were calculated graphically from the maximum of the peak to its intersection with the baseline. The calculation was performed for primary spectra.

The absolute concentrations of CO_2 and H_2O were calculated by the Beer–Lambert equation:

$$C = 100 \cdot M \cdot A_j / (d \cdot \rho \cdot \varepsilon),$$

where C is the unknown concentration of H_2O or CO_2 (wt.%), M is the molecular weight of the compound (g/mol), A_j is the intensity of the absorption peak, d is the thickness of the plate (cm), ρ is the density of the glass (g/l), and ε is the absorption coefficient (l/mol/cm).

The density of "dry" glasses was taken as 2757 g/l, according to experimental data (Shishkina et al., 2010a) for magnesian basalt of the Mutnovsky volcano in Kamchatka. The correction for a decrease in the density of glasses with increasing H_2O concentration was –22.1 g/l per 1 wt.% H_2O (Shishkina et al., 2010a). Density was calculated using H_2O contents obtained previously for the inclusions studied using an ion probe. Calculated densities of glasses varied between 2756–2689 g/l (see Table 2).

In the calculation of the CO_2 concentration, the absorption coefficient was set equal to 317 l/mol/cm and in the calculation of the total H_2O concentration (MIR), it was 68 l/mol/cm, according to experimental data (Shishkina et al., 2010a). For OH^- and H_2O_{mol}, we used absorption coefficients of 0.49 and 0.58 l/mol/cm (average), respectively, calculated by the formulas from (Ohlhorst et al., 2001):

$$\varepsilon_{OH^-} = -0.13 + 0.000257 \cdot (C_{SiO_2})^2,$$

$$\varepsilon_{H_2O} = -0.15 + 0.000304 \cdot (C_{SiO_2})^2,$$

where $(C_{SiO_2})^2$ is the SiO_2 content in the glass (wt.%).

Taking into account the measurement and the absorption coefficients estimate errors, the error in determining the H_2O and CO_2 concentrations is 10–15 rel.% (Shishkina et al., 2010a), and the detection limit of H_2O and CO_2 for the inclusions studied is estimated as 100 ppm in the MIR.

Results

H_2O in melt inclusions. The most reliable estimates of the H_2O content were obtained for a number of inclusions in the NIR by summing the concentrations of hydroxyl and molecular H_2O in the glass (see Table 2, Figs. 3 and 4). These values are consistent with data of the ion probe at the Yaroslavl Branch of the Institute of Physics and Technology (FTIAN), RAS (Yaroslavl) within an error of 15 rel.% (see Fig. 4, *a*). The largest deviation from the ion probe data is observed for the inclusion with a measured concentration of 3.97 wt.% H_2O (E312-1, see Table 2), which may be due to inaccurate calibration of the ion probe at the Yaroslavl branch of FTIAN for basaltic compositions with a high concentrations of H_2O (>2 wt.%) (Sobolev, 1996). The OH^-/H_2O ratio (average of 1.45) is close to values for experimental hydrous melts (1.8–1.6 at H_2O = 2–2.5 wt.% (Dixon et al., 1995)), indicating magmatic origin of water in studied glasses.

NIR mode is sensitive to the thickness of the sample (especially for the peak of the molecular H_2O), which must be at least 50–60 μm for reliable measurement of the absorption intensities of H_2O and OH^-. For thinner samples, the peaks are weak, which does not allow a quantitative estimate of their intensity (see Fig. 3, *c*). Because it was impossible to measure the H_2O concentration in all samples, the data of measurements in the MIR based on the intensity of the peak at 3550 cm^{-1} were also used in this work. As shown in Fig. 4, *a*, for high-water inclusions (H_2O > 1 wt.%), the H_2O concentrations measured in the MIR are underestimated up to 60 rel.% relative to the concentrations calculated from the data of the NIR and ion probe. This is due to the high intensity of the peak at 3550 cm^{-1}, the attainment of the saturation regime of the detector at high concentrations of H_2O, and, hence, an underestimation of the intensity of the absorption peak in the calculations. Low concentrations of H_2O (<1 wt.%) in the glasses measured in the MIR regime are consistent with the ion probe data within the measurement error and were used as true values (see Figs. 4, *a* and 3, *a*).

The obtained H_2O concentrations in the glasses range from 0.02 to 4 wt.%, which is in good agreement with previously published data for inclusion in high-magnesian olivine from the Kliuchevskoi volcano (Fo > 85) (Auer et al., 2009; Churikova et al., 2007; Khubunaya and Sobolev, 1998; Mironov et al., 2001; Portnyagin et al., 2007b; Sobolev and Chaussidon, 1996) (Fig. 5). The maximum value for the most primitive compositions (Fo > 89) is 2.7 wt.%. There was no correlation between the H_2O contents of the inclusion glasses and the host olivine. However, there are clear differences in H_2O content between inclusions from different types of rocks of the volcano. High-water inclusions (>2 wt.% H_2O) are typical of pyroclastic samples, and low-water inclusions (<1 wt.% H_2O) were found only in olivines from lava samples (see Table 1, Fig. 5, *a*).

CO_2 content in melt inclusions. CO_2 was measured from the intensity of the absorption peaks at 1530 and 1430 cm^{-1} (see Fig. 3, *a*, *b*). For most of the inclusions, the measurement results are identical within 15 rel.% (see Fig. 4, *b*). Noticeable

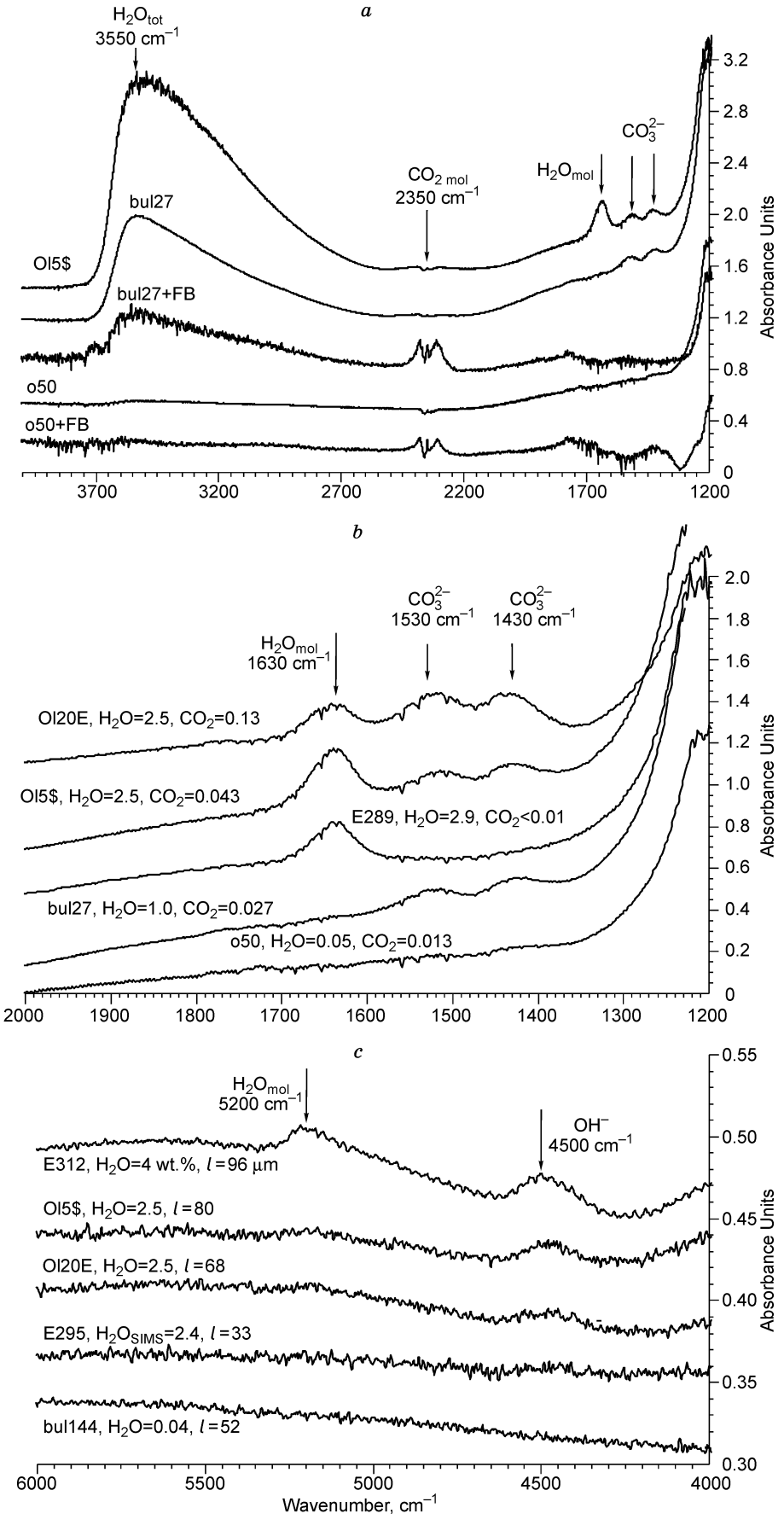
a
H2Otot
3550 cm−1
CO2 mol
2350 cm−1
H2Omol
CO3 2−
bul27
Ol5$
bul27+FB
o50
o50+FB
Absorbance Units
3700
3200
2700
2200
1700
1200
b
CO3 2−
1530 cm−1
CO3 2−
1430 cm−1
H2Omol
1630 cm−1
Ol20E, H2O=2.5, CO2=0.13
Ol5$, H2O=2.5, CO2=0.043
E289, H2O=2.9, CO2<0.01
bul27, H2O=1.0, CO2=0.027
o50, H2O=0.05, CO2=0.013
Absorbance Units
2000
1900
1800
1700
1600
1500
1400
1300
1200
c
H2Omol
5200 cm−1
OH−
4500 cm−1
E312, H2O=4 wt.%, l=96 μm
Ol5$, H2O=2.5, l=80
Ol20E, H2O=2.5, l=68
E295, H2OSIMS=2.4, l=33
bul144, H2O=0.04, l=52
Absorbance Units
6000
5500
5000
4500
4000
Wavenumber, cm−1

Fig. 3. Representative spectra of glasses of melt inclusions obtained by IR spectroscopy. *a*, Absorption spectra showing the peaks of H_2O_{tot}, CO_{2mol} and CO_3^{2-} in the mid-infrared regime (MIR). The figure shows spectra of inclusions (Ol5$, bul27, and o50) with different contents of H_2O (from top to bottom: 2.5, 1, and 0.05 wt.%) and CO_2 (0.043, 0.027, and 0.013 wt.%). For two inclusions (bul27 and o50), combined spectra of glass + fluid bubble are also given, which clearly shows the molecular CO_2 peak absent in the spectra of glasses. MI numbers are given above the spectra. *b*, Absorption spectra in the region of the carbonate doublet CO_3^{2-}. From top to bottom are shown three spectra of high-water inclusions (2.5–2.9 wt.% H_2O) containing different amounts of CO_2 and two spectra for an inclusion with moderate amounts of water and CO_2 (bul27) and for a low-water inclusion with a low content of CO_2 (o50). MI numbers and the estimated content of H_2O and CO_2 (wt.%) are given above the spectra. *c*, Spectra showing the peaks of molecular H_2O and OH obtained in the near-infrared regime (NIR). From top to bottom are shown three spectra high-water inclusions (2.5–4 wt.% H_2O) ~70–100 μm thick, for which a quantitative estimate of the total water content is possible. The 4th spectrum (E295) shows no peaks and the impossibility of estimating the water content for thin samples. The 5th spectrum (bul144) is an example of a spectrum for a low-water inclusion, in which the peaks of H_2O_{mol} and OH^- are also not identified. The names of the MIs, the estimated H_2O content (wt.%), and the thickness of the plates (*l*, μm) are given on the left above spectrum.

overestimation of the concentrations obtained from the intensity of the peak at 1530 cm^{-1} is observed only for the OL20E inclusion rich in CO_2 and H_2O (see Figs. 4, 3, *b* and Table 2), which may be due to the partial overlapping of the peak of CO_3^{2-} at 1530 cm^{-1} and the peak of molecular H_2O at 1630 cm^{-1} in this spectral range. The data obtained for the peak of CO_3^{2-} at 1430 cm^{-1} were used as true concentrations to eliminate the effect of the absorption peak of molecular H_2O on the CO_2 measurement (see Table 2).

The CO_2 variations in the studied glasses were 0.13 to <0.01 wt.% (see Table 2, Fig. 6, *a*). Similar results were also obtained in (Auer et al., 2009) for glasses of naturally quenched high-water natural inclusions in magnesian olivine compositions of ($Fo_{85.1–88.3}$) (see Fig. 6, *a*). There was no correlation between the CO_2 content and the composition of the host olivine (Fo). A systematic difference between the experimentally partially homogenized inclusions and naturally quenched inclusions was not found although the statistics for the latter is small (three measurements of CO_2). In inclusions with a high H_2O content from pyroclastic rocks, the CO_2 content is somewhat higher than that in low-water inclusions from lavas (0.033 and 0.017 wt.% on average, respectively). The maximum content of CO_2 (0.13 wt.%) was measured in the glass of one of the water-rich inclusions (OL20E, see Table 2, Fig. 6) which was quenched in the experiment at the highest temperature of 1250 °C, which was 50–100 °C higher than the quenching temperature of other inclusions.

Combined spectra of glasses and gas bubbles indicate the constant presence of molecular CO_2 in the gas phase of the inclusions (see Fig. 3, *a*).

Estimates of pressure from the composition of inclusions. The data on the H_2O and CO_2 contents in inclusion glasses allow one to estimate the equilibrium pressure between the melts and the fluid using data on the solubility of the volatile compounds under different *P–T* conditions (Neuman and Lowenstern, 2002; Shishkina et al., 2010a). For high-water inclusions the obtained estimates of the pressures range from 90 to 270 MPa (for most MIs, 100–150 MPa), and for low-water inclusions, they are less than 100 MPa (see Table 2, Fig. 7).

The crystallization pressure estimated from measured densities of the fluid inclusion is 520–550 MPa at *T* =

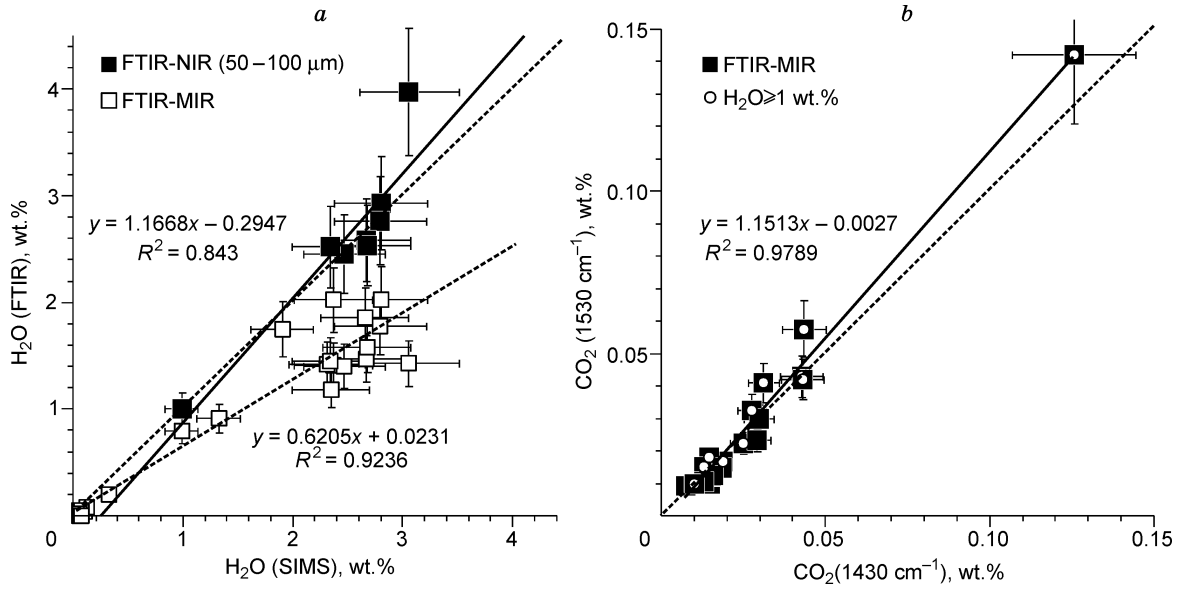

Fig. 4. Comparison of water contents estimated by IR spectroscopy (FTIR) and secondary ion mass spectrometry (SIMS). *a*, Comparison of the data obtained in the present study using FTIR in the NIR and MIR with ion probe data (SIMS) (Churikova et al., 2007; Portnyagin et al., 2007b). All SIMS data were obtained on the Cameca ims4f at the Yaroslavl Branch of FTIAN (Russia, Yaroslavl); *b*, comparison of CO_2 concentrations calculated from the intensities of the absorption peaks of CO_3^{2-} at 1430 and 1530 cm^{-1}. The figure shows the maximal measurement error equal to ±15 rel.%.

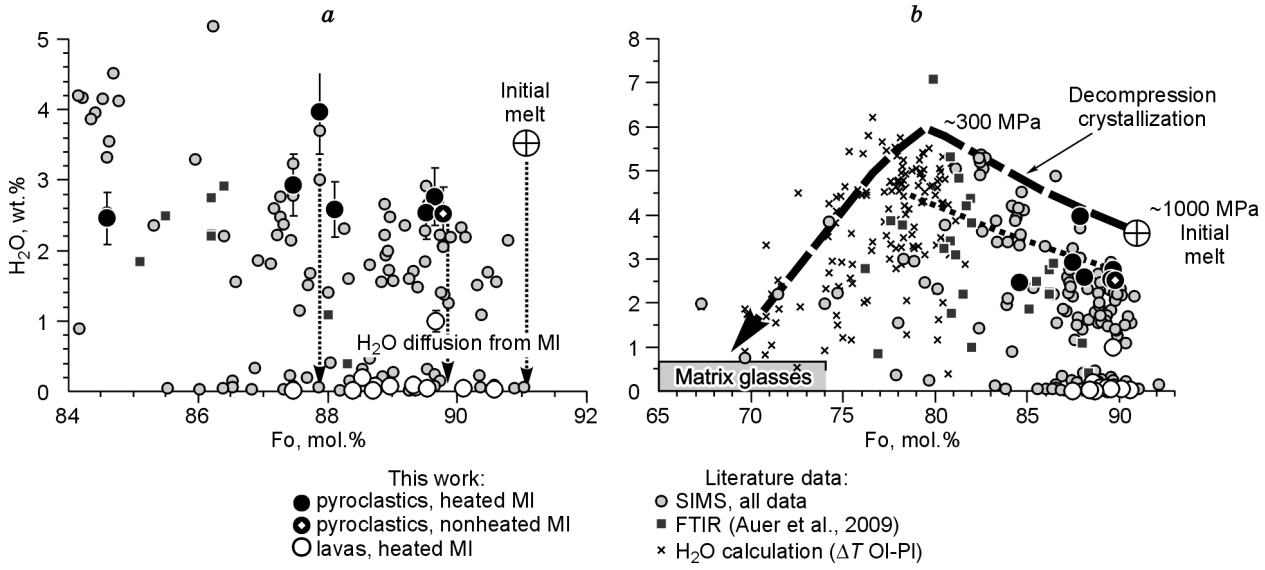

Fig. 5. Water contents in melt inclusions versus composition of the host olivine (Fo). *a*, The range of the compositions studied; *b*, the whole range of compositions of melt inclusions in olivine for the Kliuchevskoi volcano. Gray circles show previous SIMS data (Churikova et al., 2007; Khubunaya and Sobolev, 1998; Mironov, 2009; Portnyagin et al., 2007b; Sobolev and Chaussidon, 1996). The figure also shows the FTIR data of (Auer et al., 2009) for naturally quenched inclusions and calculated water contents in olivine for MI Fo < 82 (sidelong cross) obtained using the model of (Danyushevsky et al., 1996). In part *a* the dotted line shows the effect of the diffusion of H_2O from inclusions. In part *b* the dashed and dotted lines show the trends of fractionation of Kliuchevskoi volcano magmas: the dashed line refers to an initial content of 3.6 wt.%, and the dotted line to an initial content of 2.8 wt.%. In the composition range from olivine to $Fo_{91–80}$, the trends were calculated for the case of a closed crystallization system with the accumulation of H_2O in the melt ($H_2O = H_2O°/[1 – F]$) on the basis of the relationship between the degree of fractionation (F) and the composition of olivine (Fo): $F = 1 – \exp [–0.0448 \cdot (91 – Fo)]$ (Mironov, 2009; Mironov and Portnyagin, 2008). Upon reaching equilibrium between the compositions and Fo_{80} olivine, H_2O begins to degas from the melt (Mironov et al., 2001). Estimates of the pressure at various stages of crystallization were made on the basis of the data in Fig. 7.

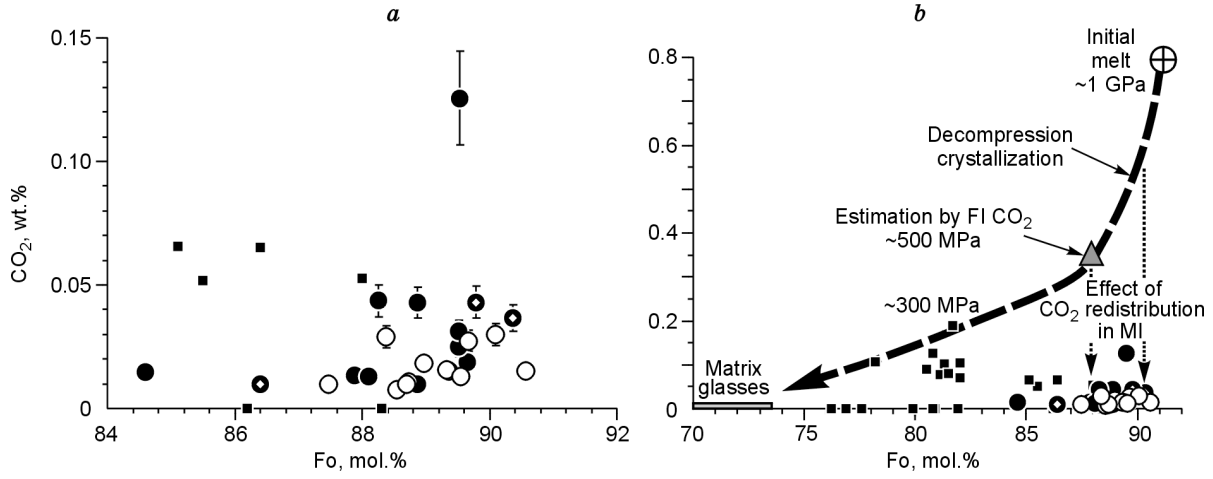

Fig. 6. CO_2 content in glasses of melt inclusions versus composition of olivine (Fo). *a*, The range of the compositions studied; *b*, the whole range of compositions of melt inclusions in olivine for the Kliuchevskoi volcano based on this work and (Auer et al., 2009). For notation see Fig. 5. In part *b*, triangle shows the CO_2 content in the melt (~0.35 wt.% at 500 MPa), estimated from the density of fluid inclusions of CO_2. The thick dashed line shows the estimated trend of the evolution of melt compositions during decompression of magma crystallization of the Kliuchevskoi volcano; the dotted line shows the effect of CO_2 redistribution between the fluid and melt in melt inclusions. Estimates of the pressure at various stages of crystallization were made using the data of Fig. 7.

1200–1250 °C. This, in turn, allows the CO_2 content in the equilibrium melt to be estimated as ~0.35 wt.% (Shishkina et al., 2010a). The results show that the studies of syngenetic melt and fluid inclusions give quite different estimates of crystallization pressure and CO_2 concentrations in melts.

Discussion

Evidence of diffusion of H_2O from melt inclusions. The inclusions studied in this work contain H_2O in amounts that differ by more than two orders of magnitude (from 0.02 to

4 wt.%). Because these contents do not correlate with the composition of the host olivine and glasses of MIs, they can hardly be associated with variations in the composition of the magma that existed in nature. The presence of dry magmas among the parental magmas of the Kliuchevskoi volcano is also difficult to explain, given the typical fractionation of these magmas to high-alumina compositions in equilibrium with olivine, pyroxene, and plagioclase only at elevated partial pressures of H_2O (Ariskin et al., 1995; Sisson and Grove, 1993).

A more likely explanation for the wide variations in the H_2O content in the MIs studied is the loss of the volatile component of the inclusions during their evolution after the entrapment of in the host mineral (Danyushevsky, 2002; Portnyagin et al., 2008). The absence of a significant difference in H_2O content between glassy and experimentally quenched MIs (see Fig. 5, *a*) indicates that short-duration experiments on partial homogenization had no significant effect on the H_2O content in the inclusions, whose must be associated with natural processes.

Undoubted evidence of H_2O loss from the investigated inclusions in nature is the correlation of its content with the type of rocks that contained the inclusions. All melt inclusions from slowly cooled lava samples contain less than 1 wt.% H_2O. Inclusions from relatively rapidly quenched samples of pyroclastic material (bombs and scoria) contain more than 2 wt.% H_2O (see Fig. 5). Consequently, the loss of H_2O from the inclusions most likely occurred during and after the eruption of magmas during their cooling at atmospheric pressure. This conclusion is consistent with the data of a study (Lloyd et al., 2010), in which a significant difference in the H_2O content in the inclusions was observed even for the pyroclastic rocks of different sizes. According to (Lloyd et al., 2010), inclusions from 6–7 cm volcanic bombs which cooled to the melt-to-glass transition temperatures for 5–10 min contained up to 1 wt.% less H_2O than inclusions from ash and up to 2 cm lapillies which cooled for less than 2 min. These data indicate that almost all inclusions studied in this work undergone loss of H_2O during cooling, which could be 1 wt.% for inclusions from pyroclastic rocks and up to 3–4 wt.% for inclusions from lavas.

Further evidence of the loss of H_2O from all inclusions studied is their behavior during the homogenization experiments, in which none of the inclusions studied was completely homogenized at the expected liquidus and superliquidus temperature of these melts. The effect of H_2O loss from inclusions on a significant increase in homogenization temperatures or the absence of homogenization has been discussed earlier (Danyushevsky et al., 2002; Sobolev and Danyushevsky, 1994). These studies have shown two main reasons for this effect. On the one hand, H_2O loss causes an increase in the equilibrium liquidus temperature of the melt and olivine and crystallization of olivine on the walls of the inclusion. On the other hand, during H_2O loss by the melt, the component with a large molar volume (~23 cm^3/mol (Ochs and Lange, 1999)) has a significant effect on the increase in the density of the residual melt and decrease in the pressure in the inclusions. The effect on the melt density is probably the greatest for inclusions trapped at relatively low pressures (Danyushevsky et al., 2002; Sobolev and Danyushevsky, 1994). Thus, according to the model of (Ochs and Lange, 1999), the effect of loss of 1 wt.% H_2O from a basaltic melt at 100 MPa should lead to a 2.5 rel.% decrease in the density of the melt. These theoretical calculations are fully consistent with our experimental dependences between the size of gas bubbles in inclusions and the H_2O content in the glasses (see Table 1) and with the low pressures in the inclusions that lost the maximum amount of H_2O (see Fig. 7).

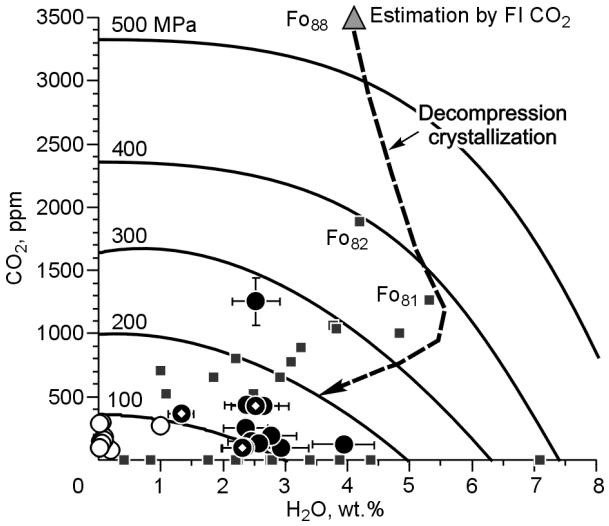

Fig. 7. H_2O and CO_2 contents in glasses of melt inclusions. For notation see Fig. 5. Isobars of saturation of the melts with the H_2O–CO_2 fluid are shown according to experimental data (Shishkina et al., 2010a). In contrast to the widely used model (Newman and Lowestern, 2002), the experimental data (Shishkina et al., 2010a), obtained for compositions close to Kliuchevskoi volcano magmas show a higher solubility of CO_2 at pressures above 100 MPa and an insignificant effect of H_2O on the solubility of CO_2 at a H_2O content of 0 to 4 wt.%. Comparison of pressure estimates by the VolatileCalc program (Newman and Lowestern, 2002) and the data of (Shishkina et al., 2010a) are listed in Table 2. The thick dashed line shows the estimated trend of the evolution of melt compositions during decompression crystallization of Kliuchevskoi volcano magmas.

The possibility of an almost complete loss of H_2O from MIs has been discussed previously (Portnyagin et al., 2008), and it has been shown based on experimental data that the loss of H_2O from MIs is probably due to the diffusion of molecular H_2O along dislocations in olivine. In contrast to the mechanism of H_2O loss from inclusions by its dissociation, hydrogen diffusion from the inclusion, and the binding of excess oxygen by oxidation of FeO in the melt, which has been assumed previously (Sobolev and Danyushevsky, 1994), the magnitude of H_2O loss by its diffusion in the molecular form is not limited by Fe^{2+} in the melt. It is likely that the diffusion of molecular H_2O can also explain the significant variations of H_2O in the MIs of the Kliuchevskoi volcano described in this paper.

Redistribution of CO_2 between the phases in melt inclusions. In contrast to H_2O, the varying CO_2 contents in MIs, which are considerably lower than those expected from

the study of FIs, cannot be attributed to diffusion through the host olivine. Evidence of this is the good preservation of high-density fluid CO_2 inclusions in olivine from samples of slowly cooling lavas. A more likely process leading to CO_2 depletion of the residual glasses is a redistribution of CO_2 between the melt and fluid phase within the inclusions. The presence of CO_2 in both the glasses and the fluid phase of the inclusions is supported by IR spectroscopy data (see Fig. 3, *a*).

The depletion of CO_2 from the residual glasses of MIs has been debated in the literature and is primarily associated with the formation of a fluid phase in an inclusion upon cooling and crystallization of the host mineral on the walls of the inclusion (Anderson and Brown, 1993). As shown by (Cervantes et al., 2002), a gas bubble of 3 vol.% in inclusions subjected to cooling to about 100 °C can contain up to 80% of the initial total content of CO_2 in the inclusion. In the case of the inclusions from Kliuchevskoi volcano rocks, this process could also occur. The efficiency of heating the inclusions for the dissolution of CO_2 from the fluid into the melt is clearly illustrated by the maximum measured concentrations of CO_2 in the OL20E inclusion (0.13 wt.%), quenched at the highest temperature (see Table 2).

Along with crystallization in the inclusions, an important factor (in this case, probably the prime factor) in the depletion of CO_2 in the glass inclusions could be a loss of H_2O from the inclusions, which has not been previously discussed in the literature. As noted above, H_2O loss from inclusions leads to a significant reduction in pressure in the inclusions, resulting not only in the impossibility of complete homogenization of the inclusions, but also in a reduction the solubility of CO_2 in the equilibrium melt and the redistribution of CO_2 from the melt into the fluid phase in the inclusion. For this reason, the glasses of partially homogenized inclusions from lavas that have almost completely lost the initial amount of H_2O contain the lowest CO_2 concentrations and have the lowest internal pressure (see Fig. 7), and inclusions from pyroclastic rocks have higher CO_2 concentrations (Figs. 6 and 7) and higher internal pressures, although the amount of olivine melted in the experiment (proportional to the MgO content in the glasses) is approximately the same in both cases (see Table 1). These observations suggest that differences in CO_2 content in glasses of the inclusions studied are associated with a redistribution of this volatile component between the gas phase and the melt in the inclusions and do not represent the compositions of the melts initially trapped in olivine.

We also note that the maximum of the currently measured CO_2 concentrations (up to 0.2 wt.%) and H_2O (5–5.5 wt.%) in melt inclusions in olivine form the Kliuchevskoi volcano were obtained for the same pyroclastic samples of the initial phase of volcanic activity with an age of about 7 thousand years (Auer et al., 2009; Mironov, 2009). Probably, these samples characterize magmas that rose to the surface especially rapidly and were efficiently quenched during eruption. Inclusions from these samples did not lose the initial H_2O content and experienced short-term cooling before eruption, which favored the retention of high CO_2 concentrations in the glasses.

Thus, the glasses of the melt inclusions analyzed provide information only on the lowest possible CO_2 concentrations in the parental magmas. Most of the CO_2 initially dissolved in the melt is in the fluid phase of the inclusions; quantitative analysis of this phase is difficult because of its low density. The lack of reliable computational models makes it impossible to obtain even a rough estimate of the total composition of the inclusions based on the CO_2 concentration in the glass and the volume of the fluid phase after quenching. In this case, the easiest method of obtaining an independent estimate of CO_2 in the parental magmas is to study fluid inclusions.

H_2O and CO_2 contents in the parental magma. Analysis of the results leads to the conclusion that the measured H_2O and CO_2 contents in the inclusions provide information about the lowest possible concentrations of these volatile components in the parental magmas of the Kliuchevskoi volcano. What were the actual concentrations of these petrologically important volatiles in magmas and sources of the Kliuchevskoi volcano?

Based on the results for the most primitive inclusions, the minimum H_2O content in the initial (equilibrium with Fo_{91} olivine) magmas is estimated at about 2.5 wt.%, which is consistent with previously published results (Khubunaya and Sobolev, 1998; Portnyagin et al., 2007a,b; Sobolev and Chaussidon, 1996). However, as shown in Fig. 5, *b*, the initial content of H_2O is 2.5 wt.% and its accumulation during melt crystallization can explain neither the composition of the E312-1 inclusion in Fo_{88} olivine, which contains 4 wt.% H_2O, nor the composition of many inclusions with 5–6 wt.% H_2O in less magnesian olivines of the Kliuchevskoi volcano ($Fo_{82–85}$). To explain the high H_2O content in these differentiated inclusions, its initial contents in magmas should be about 3.5 wt.% (see Fig. 5, *b*). Therefore, primitive MIs studied in this paper could lose about 1 wt.% H_2O upon cooling in nature, according to the data of (Lloyd et al., 2010).

Independent estimates of CO_2 in magmas were made by calculating the concentrations in melts that would be in equilibrium with CO_2-rich fluid inclusions at pressures of 500 MPa. These estimates based on experimental data (Shishkina et al., 2010a) are about 0.35 wt.% (see Figs. 6, *b* and 7). However, fluid inclusions were studied in Fo_{88} olivine, which was crystallized from more differentiated magmas than the presumed parental Kliuchevskoi melts in equilibrium with Fo_{91} olivine. Since the crystallization of magmas of the Kliuchevskoi volcano probably occurred at decompression (Ariskin et al., 1995; Mironov, 2009; Mironov and Portnyagin, 2008), the parental magmas could crystallize at high pressure and had greater concentrations of CO_2 than their differentiates.

If we assume that the H_2O/CO_2 ratio for the Kliuchevskoi volcano corresponds to the average value for the emission of volatiles from all island-all volcanoes of the Earth (H_2O/CO_2 = 4 (Wallace, 2005)), then the estimated value of CO_2 in the parental magmas reaches 0.8–0.9 wt.%. This concentration corresponds to equilibrium pressures above 900 MPa for basaltic melts similar in composition to Kliuchevskoi volcano magmas (Shishkina et al., 2010b). In this case, we must

assume that the original magmas were saturated with a mixed H_2O–CO_2 fluid even at the Moho under the Kliuchevskoi volcano (30–40 km (Balesta, 1981)) and fractionated with a continuous decrease in CO_2 in the melt (see Figs. 6, *b* and 7).

The estimates of 3.5 and 0.8–0.9 wt.% for the initial H_2O and CO_2 concentrations, respectively, in magmas of the Kliuchevskoi volcano need to be confirmed by direct measurements. For H_2O, it seems promising to use an approach based on finding primitive inclusions in samples of rapidly quenched ash. Determination of CO_2 in the parental melts requires complete experimental homogenization of the most primitive melt inclusions at high pressures.

Applications of the results. Previously, Portnyagin et al. (2007b) used the relation between the H_2O content in the primary magmas of the Kliuchevskoi volcano and the estimated degree of melting of the mantle source to estimate the temperature of magma formation (Fig. 8). The conclusion of that study was that the parental magmas of the Kliuchevskoi volcano formed at temperatures close to the dry peridotite solidus at 1.5–2.0 GPa. New estimates of H_2O content in the parental magmas enable us to refine the previous results. As shown in Fig. 8, the initial contents of H_2O = 3.5 wt.% imply, in accordance with the model (Portnyagin et al., 2007b), that the temperature of the mantle source was 40 °C below the dry peridotite solidus and that the H_2O content in the source was about 0.4 wt.%. On the one hand, this shows that the parental magmas of the Kliuchevskoi volcano had lower temperature than the sources of magmas of the Eastern volcanic front (Portnyagin et al., 2007b). The unusually high concentrations of H_2O in the source at depths of 160 km from the volcano to the subducting can suggest that the subduction of the Emperor volcanic mountain chain indeed could be the cause of the unusually hydrated source of the Kliuchevskoi volcano and its high productivity (Dorendorf et al., 2000).

The parental magmas of the Kliuchevskoi volcano were probably saturated with a H_2O–CO_2 fluid even at depths of 30–40 km, and their subsequent evolution was accompanied by simultaneous crystallization and degassing. The presumed trend of the evolution of the H_2O content in melts is shown in Fig. 5, *b*. During crystallization at depth, H_2O behaved as an incompatible element and accumulated in the melt. About 40–50% of the fractionation of the original magma at depth of 30–10 km lead to the accumulation of H_2O in the melt up to 6–7 wt.% and the formation of high-alumina magmas, prevailing among the products of the Kliuchevskoi volcano (Khrenov, 1989). The further evolution of the melts involves decompression crystallization of the magmas as they rise to the surface. H_2O contents in the magmas reached saturation at this stage (~Fo_{80}), which led to the separation the essentially aqueous fluid from the magmas, a decrease in H_2O in the melts, and abundant crystallization of plagioclase (Mironov et al., 2001). CO_2 contents in the melt probably decreased over the entire range of magma crystallization (see Fig. 6, *b*). However, it is currently difficult to estimate the exact trajectory of degassing of the magmas in the coordinates H_2O–CO_2–pressure–equilibrium composition of the fluid (see Fig. 7), especially at pressures below 300 MPa because data

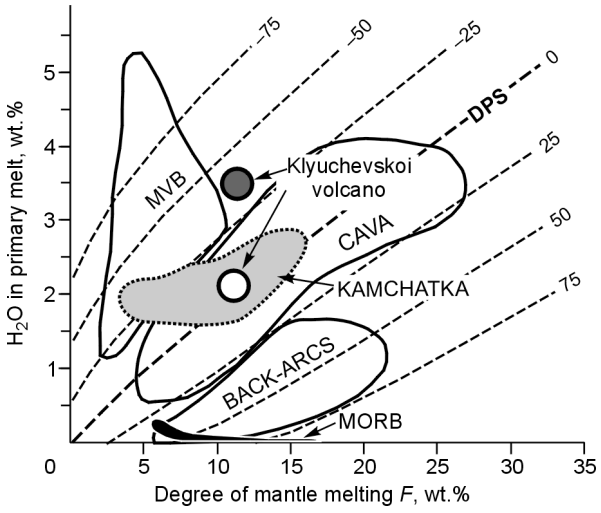

Fig. 8. Relationships between the degree of melting of peridotite (*F*) and H_2O content in primary magmas at different melting temperatures. Previous and new estimates for Kliuchevskoi volcano magmas are shown with empty and filled circles, respectively. Dashed lines show the deviation of the melting temperatures from the dry solidus of mantle peridotite (DPS) according to (Portnyagin et al., 2007b). New data on the content of volatiles in the primary melts of the Kliuchevskoi volcano indicate that they can be obtained at a temperature about 40 °C lower than the DPS (1235–1290 °C at 1.5–2.0 GPa) and H_2O contents in the mantle source of about 0.4 wt.%. Estimates of the degree of melting of the source of the Kliuchevskoi volcano and the ranges of compositions of the primary magmas of Kamchatka, MORB, basalts of back-arc basins (BACK-ARCS), Central American (CAVA) and Mexico (MVB) volcanic belts are shown according to the data of (Portnyagin et al., 2007b).

on the composition of melt inclusions are available mostly for compositions that were more or less modified by later processes and do not reflect the composition of magmas that actually existed in nature.

Conclusions

Primitive melt and fluid inclusions in olivine ($Fo_{85–91}$) from Kliuchevskoi volcano rocks were studied by experimental (high-temperature experiment and cryometry) and analytical (IR spectroscopy) methods. The variations of H_2O and CO_2 contents in the inclusions were 0.02–4 wt.% and <0.01–0.13 wt.%, respectively. Based on these results, it is concluded that the measured concentrations do not correspond to the initial compositions of the inclusions, which were modified by later processes. All the inclusions lost H_2O as a result of diffusion through the host olivine during eruption and cooling of the rocks. Almost complete loss of H_2O is characteristic of inclusions from lavas. Inclusion from pyroclastic rocks (bombs and scoria) could lose up to 1 wt.% H_2O. The low CO_2 content in the glasses and low pressures in the inclusions is attributed to the redistribution of CO_2 between the melt and fluid phase in the inclusions, which occurs after their entrapment in olivine and significantly increases as H_2O is lost from the inclusions. The minimum estimate of the CO_2 content in the primitive melts was obtained from studies of fluid

inclusions in Fo_{88} olivine, and it is 0.35 wt.% at 500 MPa and 1200–1250 °C.

The estimated H_2O and CO_2 contents in the parental magmas of the Kliuchevskoi volcano are 3.5 and 0.35–0.9 wt.%, respectively. The data obtained provide a better understanding of the origin conditions of primary magmas and serve as a basis for modeling their evolution in crust. Crystallization of Kliuchevskoi volcano magmas occurred under decompression and was accompanied by separation of the H_2O–CO_2 fluid of variable composition from the magmas.

Acknowlegements. We thank R.E. Botcharnikov and T.A. Shishkina (Institute of Mineralogy at the Leibniz University, Hannover, Germany) for help and advice in the study of melt inclusions by IR spectroscopy, F. Holtz and H. Behrens for providing possibility to perform FTIR studies in Hannover, V.B. Naumov (GEOKHI, RAS) for assistance in the study of fluid inclusions, and P.Yu. Plechov, S.A. Khubunaya and G. Werner for providing samples for research. We are grateful to P.Yu. Plechov (Moscow State University) and V.V. Sharygin (IGM, SB RAS) for their comments and constructive suggestions on the previous version of this article.

This work was supported by RFBR (grant no. 09-05-01234) and the KALMAR Russian-German project funded by the Ministry of Science and Education of Germany and a Russian President grant for leading Russian scientific schools (NSh-3919.2010.5).

References

Anderson, A.T., Brown, G.G., 1993. CO_2 contents and formation pressures of some Kilauean melt inclusions, Am. Mineral. 78, 794–803.

Ariskin, A.A., Barmina, G.S., Ozerov, A.Yu., Nielsen, R.L., 1995. Genesis of high-alumina basalts from Klyuchevskoi volcano. Petrology 3 (5), 449–472 [translated from Petrologiya 3 (5), 496–521].

Auer, S., Bindeman, I., Wallace, P., Ponomareva, V., Portnyagin, M., 2009. The origin of hydrous, high-delta O-18 voluminous volcanism: diverse oxygen isotope values and high magmatic water contents within the volcanic record of Klyuchevskoi volcano, Kamchatka, Russia. Contrib. Mineral. Petrol. 157 (2), 209–230.

Balesta, S.T., 1981. The Earth's Crust and Magma Chambers in the Areas of Modern Volcanism [in Russian]. Nauka, Moscow.

Braitseva, O.A., Melekestsev, I.V., Ponomareva, V.V., Sulerzhitsky, L.D., 1995. Ages of calderas, large explosive craters and active volcanoes in the Kuril-Kamchatka region, Russia. Bull. Volcanol. 57 (6), 383–402.

Calkins, J., 2004. $^{40}Ar/^{39}Ar$ geochronology of Khapitsa plateau and Studyonaya river basalts and basaltic andesites in Central Kamchatka Depression, Kamchatka, Russia, in: Relationship between Tectonics, Seismicity, Magma and Volcanic Eruptions in the Volcanic Arcs (Proceedings of IV International Workshop on Subduction Processes in the Kurile-Kamchatka-Aleutian Arcs, Petropavlovsk-Kamchatskii, 21–27 August 2004).

Carroll, M., Holloway, J.R. (Eds.), 1994. Volatiles in Magmas. Rev. Mineral., Vol. 30.

Cervantes, P., Kamenetsky, V., Wallace, P., 2002. Melt inclusion volatile contents, pressures of crystallization for Hawaiian picrites and the problem of shrinkage bubbles. EOS Trans. AGU 83 (47), Fall Meet. Suppl., Abstract V22A-1217.

Churikova, T., Worner, G., Mironov, N., Kronz, A., 2007. Volatile (S, Cl and F) and fluid mobile trace element compositions in melt inclusions: implications for variable fluid sources across the Kamchatka arc. Contrib. Mineral. Petrol. 154 (2), 217–239.

Danyushevsky, L.V., Sobolev, A.V., Dmitriev, L.V., 1996. Estimation of the pressure of crystallization and H_2O content of MORB and BABB glasses: calibration of an empirical technique. Mineral. Petrol. 57 (3–4), 185–204.

Danyushevsky, L.V., McNeill, A.W., Sobolev, A.V., 2002. Experimental and petrological studies of melt inclusions in phenocrysts from mantle-derived magmas: an overview of techniques, advantages and complications. Chem. Geol. 183, 5–24.

Dixon, J.E., Stolper, E.M., Holloway, J.R., 1995. An experimental study of water and carbon dioxide solubilities in mid ocean ridge basaltic liquids. Part I: Calibration and solubility models. J. Petrol. 36 (6), 1607–1631.

Dorendorf, F., Wiechert, U., Worner, G., 2000. Hydrated sub-arc mantle: a source for the Kluchevskoy volcano, Kamchatka/Russia. Earth Planet. Sci. Lett. 175, 69–86.

Fedotov, S.A., Masurenkov, Yu.P. (Eds.), 1991. Active Volcanoes of Kamchatka [in Russian]. Nauka, Moscow, Vol. 1.

Hansteen, T.H., Klügel, A., 2008. Fluid inclusion thermobarometry as a tracer for magmatic processes, in: Putirka, K.D., Tepley, F.J. (Eds.), Minerals, Inclusions and Volcanic Processes. Rev. Mineral. Geochem., Vol. 69. Mineral. Soc. Am., Chantilly, pp. 142–177.

Kersting, A.B., Arculus, R.J., 1994. Klyuchevskoi volcano, Kamchatka, Russia: the role of high-flux recharged, tapped, and fractionated magma chamber(s) in the genesis of high-Al_2O_3 from high-MgO basalt. J. Petrol. 35, 1–41.

Khrenov, A.P., Antipin, V.S., Chuvashova, L.A., Smirnova, E.V., 1989. Petrochemical and geochemical characteristics of basalts of the Klyuchevskoi volcano. Vulkanologiya i Seismologiya, No. 3, 3–15.

Khubunaya, S.A., Sobolev, A.V., 1998. Primary melts of calc-alkaline magnesian basalts from the Klyuchevskoi volcano (Kamchatka). Dokl. Akad. Nauk 360 (1), 100–102 [Dokl. Earth Sci. 360 (4), 537–539].

Khubunaya, S.A., Bogoyavlenskiy, S.O., Novgorodtseva, T.Yu., Okrugina, A.I., 1994. The mineralogy of the Klyuchevskoi magnesian basalts depicting the fractionation in the magma chamber. Volcanol. Seismolog. 15 (3) [translated from Vulkanologiya i Seismologiya, 1993, No. 3, 46–68].

Khubunaya, S.A., Gontovaya, L.I., Sobolev, A.V., Nizkous, I.V., 2007. Magma chambers beneath the Klyuchevskoy Volcanic Group (Kamchatka). J. Volcanol. Seismolog. 1 (2), 98–118 [translated from Vulkanologiya i Seismologiya, No. 2, 32–54].

Lloyd, A.S., Plank, T., Ruprecht, P., Hauri, E., Rose, W.I., 2010. Volatile loss from melt inclusions in clasts of differing sizes. Abstract V24C-04 presented at 2010 Fall Meeting, AGU, San Francisco, Calif., 13–17 Dec., 2010.

Melekestsev, I.V., 1980. Volcanism and Relief Formation [in Russian]. Nauka, Moscow.

Metrich, N., Wallace, P.J., 2008. Volatile abundances in basaltic magmas and their degassing paths tracked by melt inclusions, in: Putirka, K.D., Tepley, F.J. (Eds.), Minerals, Inclusions and Volcanic Processes. Rev. Mineral. Geochem., Vol. 69, Mineral. Soc. Am., Chantilly, pp. 363–402.

Mironov, N.L. 2009. The origin and evolution of Klyuchevskoi volcano magmas from study of melt inclusions in olivine. Candidate's Dissertation (PhD Thesis Equivalent) in Geology and Mineralogy. GEOKHI RAS, Moscow.

Mironov, N.L., Portnyagin, M.V., 2008. Dynamics of crystallization and magma transport beneath Klyuchevskoy volcano (Kamchatka), in: Proceedings of XIII International Conference on Thermobarogeochemistry and IV Symposium APIFIS, Moscow. IGEM RAS, Vol. 1, pp. 110–113.

Mironov, N.L., Portnyagin, M.V., Plechov, P.Yu., Khubunaya, S.A., 2001. Final stages of magma evolution of Klyuchevskoi volcano, Kamchatka: evidence from melt inclusions in minerals of high-alumina basalts. Petrology 9 (1), 46–62 [translated from Petrologiya 9 (1), 51–69].

Naumov, V.B., 1979. Determining the concentration and pressure of volatile components in magmatic melts based on inclusions in minerals. Geokhimiya, No. 7, 997–1007.

Naumov, V.B., 2011. Rhyolitic melts in eastern Transbaikalia and the North Caucasus: chemical composition, volatiles, and admixture elements (*from data of study of melt inclusions in minerals*). Russian Geology and Geophysics (Geologiya i Geofizika), 52 (11), 1368–1377 (1734–1745).

Naumov, V.B., Kovalenko, V.I., Dorofeeva, V.A., Girnis, A.V., Yarmolyuk, V.V., 2010. Average compositions of igneous melts from main

geodynamic settings according to the investigation of melt inclusions in minerals and quenched glasses of rocks. Geochem. Int. 48 (12), 1185–1207 [translated from Geokhimiya, No. 12, 1266–1288].

Newman, S., Lowenstern, J.B., 2002. VOLATILECALC: a silicate melt–H_2O–CO_2 solution model written in Visual Basic for Excel. Comp. Geosci. 28 (5), 597–604.

Ochs, F.A., Lange, R.A., 1999. The density of hydrous magmatic liquids, Science 283, 1314–1317.

Ohlhorst, S., Behrens, H., Holtz, F., 2001. Compositional dependence of molar absorptivities of near-infrared OH^- and H_2O bands in rhyolitic to basaltic glasses. Chem. Geol. 174, (1–3), 5–20.

Ozerov, A.Y., 2000. The evolution of high-alumina basalts of the Klyuchevskoi volcano, Kamchatka, Russia, based on microprobe analyses of mineral inclusions. J. Volcanol. Geotherm. Res. 95, 65–79.

Portnyagin, M.V., Mironov, N.L., Matveev, S.A., Plechov, P.Y., 2005. Petrology of avachites, high-magnesian basalts of Avachinsky volcano, Kamchatka: II. Melt inclusions in olivine. Petrology 13 (4), 322–351 [translated from Petrologiya 13 (4), 358–388].

Portnyagin, M., Bindeman, I., Hoernle, K., Hauff, F., 2007a. Geochemistry of primitive lavas of the Central Kamchatka Depression: magmas generation at the edge of the Pacific plate, in: Eichelberger, J., Gordeev, E., Izbekov, P., Kasahara, M., Lees, J. (Eds.), Volcanism and Subduction: The Kamchatka Region. Geophys. Monogr. Ser., Vol. 172. AGU, Washington, D.C., pp. 199–239.

Portnyagin, M., Hoernle, K., Plechov, P., Mironov, N., Khubunaya, S., 2007b. Constraints on mantle melting and composition and nature of slab components in volcanic arcs from volatiles (H_2O, S, Cl, F) and trace elements in melt inclusions from the Kamchatka Arc. Earth Planet. Sci. Lett. 255 (1–2), 53–69.

Portnyagin, M., Almeev, R., Matveev, S., Holtz, F., 2008. Experimental evidence for rapid water exchange between melt inclusions in olivine and host magma. Earth Planet. Sci. Lett. 272 (3–4), 541–552.

Shishkina, T.A., Botcharnikov, R.E., Holtz, F., Almeev, R.R., Portnyagin, M.V., 2010a. Solubility of H_2O- and CO_2-bearing fluids in tholeiitic basalts at pressures up to 500 MPa. Chem. Geol. 277 (1–2), 115–125.

Shishkina, T.A., Botcharnikov, R.E., Almeev, R.R., Holtz, F., 2010b. Magma storage conditions and degassing processes of low-K and high-Al island-arc tholeiites: Experimental constraints for Mutnovsky volcano, Kamchatka. IODP/ICDP Kolloquium, Frankfurt, Germany.

Sisson, T.W., Grove, T.L., 1993. Experimental investigations of the role of H_2O in calc-alkaline differentiation and subduction zone magmatism. Contrib. Mineral. Petrol. 113, 143–166.

Smirnov, S.Z., Sharygin, V.V., Szabó, C., 2011. Melts and fluids in natural mineral and ore formation: modern studies of fluid and melt inclusions in minerals. Russian Geology and Geophysics (Geologiya i Geofizika), 52 (11), 1283–1285 (1629–1631).

Sobolev, A.V., 1996. Melt inclusions in minerals as a source of principle petrological information. Petrology 4 (3), 209–220 [translated from Petrologiya 4 (3) 228–239].

Sobolev, A.V., Chaussidon, M., 1996. H_2O concentrations in primary melts from island arcs and mid-ocean ridges: Implications for H_2O storage and recycling in the mantle. Earth Planet. Sci. Lett. 137, 45–55.

Sobolev, A.V., Danyushevsky, L.V., 1994. Petrology and geochemistry of boninites from the north termination of the Tonga Trench: Constraints on the generation conditions of primary high-Ca boninite magmas. J. Petrol. 35, 1183–1211.

Sobolev, A.V., Slutskii, A.B., 1984. Composition and crystallization conditions of the initial melt of the Siberian meimechites in relation to the general problem of ultrabasic magmas. Geologiya i Geofizika (Soviet Geology and Geophysics), No. 12, 97–110 (93–104).

Span, R., Wagner, W., 1996. A new equation of state for carbon dioxide covering the fluid region from the triple point temperature to 1100 K at pressures up to 800 MPa. J. Chem. Ref. Data 25, 1509–1596.

Sokolova, E.N., Smirnov, S.Z., Astrelina, E.I., Annikova, I.Yu., Vladimirov, A.G., Kotler, P.D., 2011. Ongonite–elvan magmas of the Kalguty ore-magmatic system (Gorny Altai): composition, fluid regime, and genesis. Russian Geology and Geophysics (Geologiya i Geofizika), 52 (11), 1378–1400 (1748–1775).

Sterner, S.M., Pitzer, K.S., 1994. An equation of state for carbon dioxide valid from zero to extreme pressures. Contrib. Mineral. Petrol. 117, 362–374.

Wallace, P.J., 2005. Volatiles in subduction zone magmas: concentrations and fluxes based on melt inclusion and volcanic gas data. J. Volcanol. Geotherm. Res. 140 (1–3), 217–240.